Search by proteins for their DNA target site: 1. The effect of DNA conformation on protein sliding

Arnab Bhattacherjee and Yaakov Levy[*]

Department of Structural Biology, Weizmann Institute of Science, Rehovot 76100, Israel

ABSTRACT

The recognition of DNA-binding proteins (DBPs) to their specific site often precedes by a search technique in which proteins slide, hop along the DNA contour or perform inter-segment transfer and 3D diffusion to dissociate and re-associate to distant DNA sites. In this study, we demonstrated that the strength and nature of the non-specific electrostatic interactions, which govern the search dynamics of DBPs, are strongly correlated with the conformation of the DNA. We tuned two structural parameters, namely curvature and the extent of helical twisting in circular DNA. These two factors are mutually independent of each other and can modulate the electrostatic potential through changing the geometry of the circular DNA conformation. The search dynamics for DBPs on circular DNA is therefore markedly different compared with linear B-DNA. Our results suggest that, for a given DBP, the rotation-coupled sliding dynamics is precluded in highly curved DNA (as well as for over-twisted DNA) because of the large electrostatic energy barrier between the inside and outside of the DNA molecule. Under such circumstances, proteins prefer to hop in order to explore interior DNA sites. The change in the balance between sliding and hopping propensities as a function of DNA curvature or twisting may result in different search efficiency and speed.

INTRODUCTION

The most intriguing aspect of protein–DNA interactions is that DNA-binding proteins (DBPs) can rapidly search and specifically recognize target DNA sites (their cognate sites) among an astronomically large number of non-specific DNA sequences (1–3). The fast association rate (even faster than the rate estimated for three-dimensional (3D) diffusion-limited reactions) may originate from strong electrostatic attractions between the searching protein and the DNA as well as from reduction of dimensionality of the search for the target (4,5). The latter led to the idea of facilitated diffusion (6,7), during which DBPs lower the dimension of their search space by performing one-dimensional (1D) diffusion along the DNA contour ('sliding') interspersed by 3D dissociation. The 3D events can further be considered as a combination of dissociation–reassociation events of short life spans ('hopping'), inter-segmental 'jumps' between nearby DNA segments and larger volume 3D diffusions.

This multifaceted protein search dynamics along the DNA contour has been indirectly studied by investigating DNA cleavage using restriction enzymes or DNA repair enzymes in bulk assays, measuring association times as a function of DNA length and monitoring the processivity with inter-site spacing (8–16). Direct evidence, however, came with advancements in nuclear magnetic resonance (NMR) spectroscopy and single molecule techniques that enabled visualization of the 1D diffusion of a protein along DNA (10,17–21). Furthermore, in a series of NMR experiments, Clore *et al*. (22–24) demonstrated that proteins perform a spiral motion along the major grooves of the DNA while interacting non-specifically with it via electrostatic attractions between commonly occurring positively charged patches on the DBPs (25) and the negatively charged backbone of the DNA. These results are consistent with our study to probe the structural and dynamic features of proteins on a single B-DNA using coarse-grained computational models (26). Other *in silico* studies using various computational approaches have also provided many other important insights regarding protein–DNA interactions, such as the effects of conformational flexibility and the sequence composition of proteins on interactions with DNA, the mechanisms used by multimeric proteins to scan DNA sequences and the impacts of crowding agents attached to genomic DNA that often function as obstacles in the path of DBPs (27–37).

Despite the considerable advancements made in understanding the molecular interactions that underpin protein search dynamics on DNA molecules (38–43), the impact of DNA conformation on the same is less explored (44–47). Often DNA molecules are assumed to have the ideal B-DNA geometry and to behave like a charged rigid rod in *in*

*To whom correspondence should be addressed. Tel: +972 8 934 4587; Fax: +972 8 934 4136; Email: Koby.Levy@weizmann.ac.il
Present address: Arnab Bhattacherjee, Indraprastha Institute of Information Technology (IIIT), New Delhi 110020, India.

slico experiments. Examples of deformed DNA structures are, however, abundant in nature. For example, the DNA molecule switches conformation while binding with the sex determining region Y (SRY) protein (48,49). On a global scale, evidence shows that DNA is overstretched one and half times compared with ideal B-DNA in the RecA filament, which is a polymeric protein–DNA complex (50). On a more local scale, bending, kinks and supercoiling in the DNA structure were found to play important roles in packing, gene expression, protein synthesis (51,52) and *in vivo* protein transport (20). Furthermore, even nuances in DNA conformations can remarkably change its affinity to proteins (53–55). It was suggested that these altered DNA conformations may accelerate the association kinetics (56) and affect many subtle molecular details (known as direct and indirect readouts), including the formation of hydrogen-bond networks in specific protein–DNA complexes (57,58). However, it remains unclear how the geometry of DNA conformations impacts the protein search dynamics, which is driven primarily by non-specific interactions. Do DBPs adopt different search mechanisms to scan geometrically different DNA conformations? If so, how does this affect the search efficiency and how significant is the effect?

In this article, we probe these issues by generating two geometrically different sets of circular DNA conformations having: (1) various DNA curvatures and (2) different degrees of twisting in the DNA double helix. We pair each of these DNA structures with a DBP and perform coarse-grained molecular dynamics simulations to investigate the molecular details of the search mechanism. The selection of circular DNA as the test bed is inspired by the fact that this form of DNA is quite common, typically found in bacterial DNA and the cytoplasmic DNA of animals. In addition, giant DNA molecules in higher organisms often form loops, held together by protein fasteners, in which each loop is largely analogous to closed circular DNA. We found that at the limit of low salt concentrations, where the protein preferably exists in a bound state with the DNA molecule, the geometry of the latter largely controls the strength of non-specific interactions between the protein and DNA and thereby modulates the search efficiency and dynamics of DBPs.

MATERIALS AND METHODS

Simulation protocol

The molecular nature of the dynamics of protein search on DNA was studied using a coarse-grained model (25,26) in which the protein is represented by a single bead per residue centered at the C_α position and the double-stranded DNA is modeled by three beads per nucleotide (representing phosphate, sugar and base) that are positioned at the geometric center of the represented group. A negative point charge is placed on each bead representing Asp or Glu amino acid residues and the DNA phosphate groups, whereas a unit positive charge is placed on each Arg and Lys residue.

To isolate the effect of DNA conformations on the dynamics of DBPs, we used DNA structures with various geometries that were held fixed throughout the simulation while the searching protein was internally flexible and completely dynamic (26,59,60). The DNA molecule was placed

at the center of a cubic box with periodic boundary conditions such that the DNA was 150 Å away from each of the sides of the box. The protein molecule was initially placed at a distance of 50 Å on the *X*-axis from the DNA and the time evolution of its motion along the DNA was studied through Langevin dynamics. We note that, when the size of the DNA changes, the box size and hence the effective concentrations also change. This might impact the 3D diffusion of protein. We are, however, interested in characterizing only the bound conformations of the protein–DNA complex, therefore, this problem can easily be circumvented by identifying a low salt concentration at which the protein remains associated with DNA and interacts with it. We carried out all of our simulations under such salt conditions and at a temperature at which the protein was completely folded.

The conformational energy of the protein was estimated by using a native topology-based model (61,62) that excludes non-native interactions and uses the Lennard–Jones potential to represent native contact interactions. In addition to these native interactions, electrostatic interactions between all charged residues of the protein and the phosphate beads of the DNA were included and were modeled by the Debye–Hückel potential, which accounts for the ionic strength of a solute immersed in an aqueous solution (63,64). One should note that due to the coarse-grained nature of the model, the distances between the charged beads of the protein and of the DNA are longer compared to the fully atomistic models. The effective electrostatic interactions are therefore weaker in our model and correspondingly the effective range of salt concentration (0.01–0.05 M) that allows the protein to interact strongly with the DNA molecule is typically lower compared to the physiological salt conditions (0.1–0.15 M) (32,65,66). Nevertheless, the model has been proven to successfully capture key characteristics of protein search modes on DNA (25,27,29) at salt conditions ranging from 0.01 to 0.2 M. We used a dielectric constant of 70–80, because the protein–DNA interface is much more hydrated in the non-specific complex than in the specific complex (39). The Debye–Hückel potential has been used previously to study the energetics and dynamics of various biomolecular systems, such as RNA folding (67–69), chromatin assembly (70) and protein–DNA binding (71,72). While the Debye–Hückel approximation is a powerful means for introducing the electrostatic screening effect of ions into the Coulomb potential, it makes several approximations, including not taking into account ion condensation on the DNA. In particular, the Debye–Hückel potential fails significantly in high ion concentration (>0.5 M) (73). However, the approximation is valid for dilute solutions of the type studied here. More details on the simulation can be found in the work of Givaty and Levy (26).

Structural annotation of the studied DBP

In all the simulations, we probed the dynamics of a human DBP Sap-1 (PDB code: 1bc8) moving along DNA conformations of various geometries. This globular protein, which is 93 amino acids long, is an Ets transcription factor and bears a total of 15 positively and 6 negatively charged residues. It uses a winged-helix DNA-binding domain to activate transcription (see Supplementary Figure S1).

DNA conformations and their characterization

To generate DNA conformations of different geometries, we used two different tools: the w3DNA (3D DNA Structure web server) [74] web server and Nucleic Acid Builder (NAB) [75]. While w3DNA accepts DNA sequences of a single DNA helix and produces a linear double-stranded B-DNA structure, NAB can be used to create a closed circular DNA duplex. The required inputs for NAB are: (1) the number of base pairs (N_{bp}) and (2) the degree of DNA supercoiling. We set N_{bp} as a multiple of 10 to maintain a uniform rise of 3.38 Å (similar to that found in ideal B-DNA) and tuned the DNA supercoiling by the number of helical twists, specified by the change in linking number, Δlk. It should be noted here that apart from the helical twisting number lk, the overall supercoiled DNA topology is also determined by the super helical twisting (writhe) number wr. In the present study, we, however, constructed DNA conformations only by varying helical twisting and the writhe number was kept constant at zero. Positive and negative Δlk values represent the number of extra turns added (so creating narrower internal groove widths) or subtracted (so creating wider internal groove widths), respectively. For example, if the original circle comprised of N_{bp}, then the number of turns in the supercoiled circle will be $N_{bp}/10 + \Delta lk$. For positive values of Δlk, we can have over-twisted DNA structures, whereas under-twisted DNA conformations correspond to negative Δlk values. In this study, we generated two sets of geometrically different circular DNA. In one, we varied the curvature of DNA circles by increasing N_{bp} but maintained a constant number of helical twist by setting Δlk to zero. In the second set, we altered the number of helical twists (i.e. various values of Δlk) but N_{bp} was fixed to 100.

We estimated the major groove widths of all the DNA conformations using the Curves web server [76].

Calculations of electrostatic potentials along the DNA contour

Electrostatic potentials were estimated by solving the nonlinear Poisson–Boltzman equation using a 0.08 M salt concentration and the DelPhi program [77]. Partial charges and atomic radii were taken from the Amber force field [78]. The interior of the molecular surface of the solute molecule (calculated with a 1.4 Å probe sphere) was assigned a dielectric constant of $\epsilon = 2$, whereas the exterior aqueous phase was assigned a value of $\epsilon = 80$. Debye–Hückel boundary conditions and five focusing steps were used with 70% of the lattice filled and the scale set to 2 grid/Å.

The electrostatic potential is measured at a reference point i, defined as the geometric midpoint between the phosphate atoms of nucleotide i in the 5′–3′ strand and nucleotide i - 4 in the 3′–5′ strand (shown as blue spheres in Figure 1A).

Sliding, hopping, 3D diffusion and the 1D diffusion coefficient

We analyzed the trajectories of the coarse-grained simulations to quantify the percentage of protein sliding, hopping and 3D diffusion used, as well as the 1D diffusion coefficient (D1) using the method previously described by Gi-

vaty and Levy [26]. To obtain sufficient statistical power, we performed 10 independent simulations of 10^8 molecular dynamics steps for each protein–DNA system. The protein was considered to be utilizing the 3D diffusion mode if the center of the recognition helix was located more than 30 Å from the center of the closest DNA base pair. At this distance, average electrostatic energy drops to about 2% of the energy in the sliding conformations at a low salt concentration, signifying an unbound state for the protein–DNA complex. A snapshot was defined as taking part in a sliding search if at least 70% of the recognition region was in contact with the DNA major groove, the distance of the center of mass of the recognition region from the center of the closest DNA base pair was up to 14 Å longer than that in the crystal structure, and the orientation angle was less than 25°. If the recognition helix was found at a distance of less than 30 Å from the DNA and did not meet any of the criteria for the sliding mode, the frame was defined as representing protein hopping along the DNA. This definition allows clear differentiation of the search mode adopted by the DBP during its interactions with the DNA while it interacts with DNA (see Supplementary Figure S2).

RESULTS AND DISCUSSIONS

In order to model the effects of DNA conformations on the sliding dynamics of DBPs, we first characterized the structural differences between a circular and an ideal linear B-DNA molecule where both comprised 100 bp. We then simulated Sap-1 searching both circular and linear DNA to study the dynamics of the DBP under various salt concentrations (Cs) and selected a suitable salt condition at which Sap-1 remains associated with both the non-specific DNA molecules. This salt concentration was used for the rest of the simulations in which the DNA geometry was modulated by two different parameters, namely the DNA curvature and degree of twisting in DNA double helix, to probe their effects on the search dynamics of the DBP.

Differences in circular and linear DNA geometry

We first generated circular and linear B-DNA structures comprising 100 bp (see Materials and Methods section) arranged in an identical sequence order (Figure 1A). In a simplified manner, the circular DNA can be visualized as being created by linking the two ends of the linear B-DNA such that the rise (10 bp per 33.8 Å) is constant. It is then interesting to investigate how simple cyclization can modulate the geometry and physical properties of the DNA. One obvious change is that, upon shifting from linear B-DNA to circular DNA, the curvature, defined as an inverse function of the radius of the DNA axis, changes from 0 to ∼0.02 per Å. Another important feature is that the width of the major groove differs between the inside ($W_{in} \sim 9.4$ Å) and the outside ($W_{out} \sim 11.5$ Å) of the circular DNA (see Figure 1B). The linear B-DNA, in contrast, exhibits a constant major groove width of $W_{B-DNA} = 10.8$ Å. The increased curvature and narrow major groove widths inside the circular DNA mean that two negatively charged phosphate atoms may lie in closer proximity to each other on circular DNA than on linear DNA. As a result, the electrostatic potential is also expected to vary between the interior and the
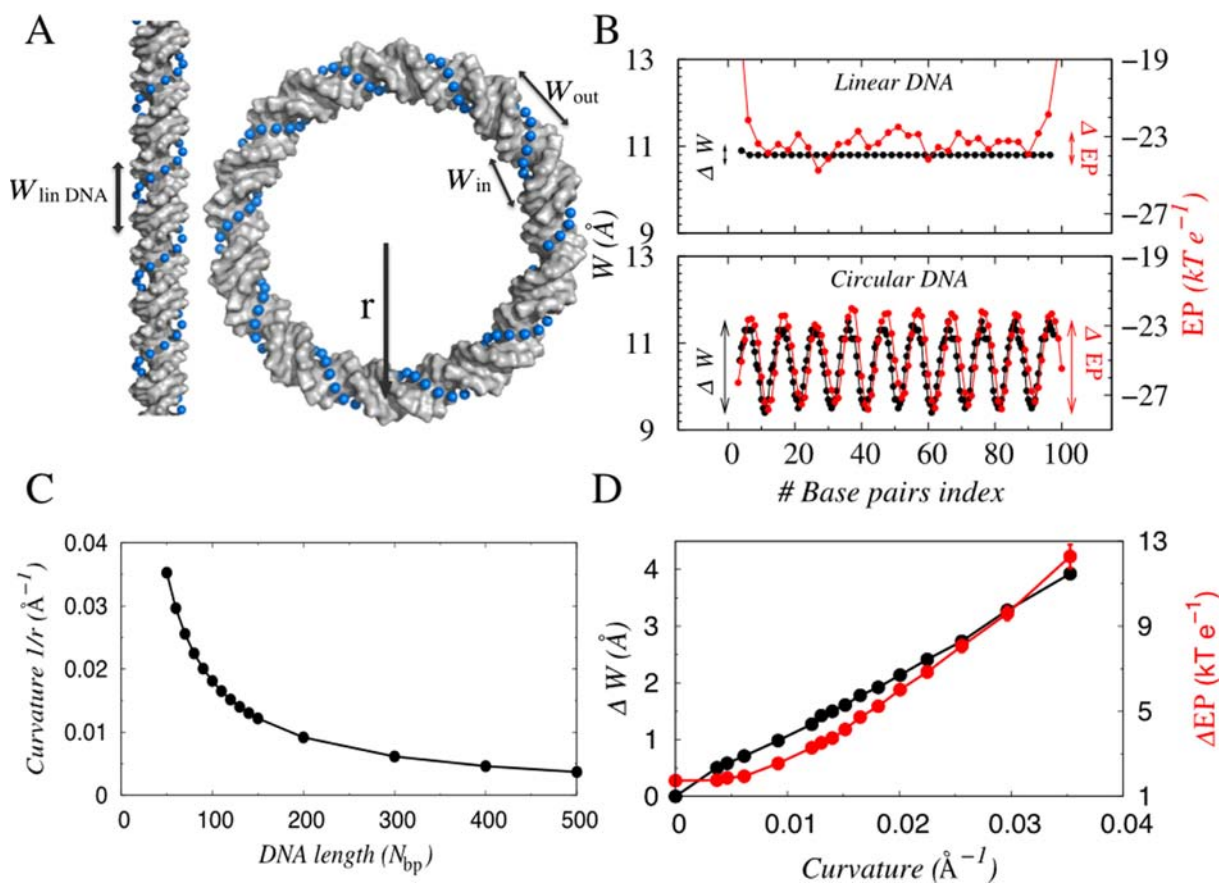
Figure 1. Structural characterization of linear (length, 100 bp) and circular (circumference, 100 bp) DNA molecules. (**A**) Conformations of an ideal B-DNA (partly shown) and circular DNA. Unlike the uniform major groove widths ($W_{B-DNA} = 10.8$ Å) observed in linear B-DNA, circular DNA shows wider major grooves on the exterior of the DNA circle (W_{out}) and narrower major groove widths inside (W_{in}) the circle. (**B**) Correlations between the major groove widths (black) and the electrostatic potential (red) for a linear (upper panel) and circular (lower panel) DNA molecule calculated at the reference points shown by the blue spheres in (A) (see Materials and Methods section for details). (**C**) Correlation between the circumference (in bp) of circular DNA and its curvature (defined as $1/r$, where r is the radius of the circular DNA). The curvature of linear DNA is 0 by definition. (**D**) Correlations between the changes in major groove width (black) and potential energy (EP; red) with the curvature of the circular DNA. The change in width and potential energy are determined by $\Delta W = W_{out} - W_{in}$ and $\Delta EP = EP_{out} - EP_{in}$.

exterior of the circular DNA molecule. Indeed, this is exactly what is obtained by solving the non-linear Poisson–Boltzmann equation using DelPhi (77), as presented in Figure 1B, which shows that the electrostatic potential of circular DNA (red line, lower panel) varies between $-22\ k_B T$ and $-27.5\ k_B T$. The oscillating trend agrees well with the periodicity of the change in major groove widths (black line lower panel) along the length of the DNA. For linear B-DNA also (upper panel), the small variation in electrostatic potential (which fluctuates around a mean of 23.5 ± 0.86 $k_B T$) is highly consistent with the flat distribution of major groove widths along the length of the molecule. This suggests a strong correlation between groove geometry and the electrostatic potential of DNA molecules.

To elaborate the effect further, we generated a set of 15 circular DNA conformations composed of 50–500 bp and present their curvatures against DNA circumference (number of base pairs) in Figure 1C. Curvature is calculated as the inverse of the DNA radius, defined as the distance between the center of mass of the DNA and the center of mass of any base pair. The results suggest that curvatures of circular DNA molecules with $N_{bp} > 100$, change slowly,

whereas the curvatures of DNA minicircles ($N_{bp} \leq 100$) increase rapidly as the number of base pairs decreases. In Figure 1D, we present the differences in major groove width ($\Delta W = W_{out} - W_{in}$) and electrostatic potential ($\Delta EP = EP_{out} - EP_{in}$) between the interior and the exterior of the circular DNA as a function of increasing DNA curvature. Both of the quantities share a linear relationship with increasing DNA curvature, which confirms the existence of a strong correlation between DNA major groove width and electrostatic potential. Any perturbation in groove width (due to a change in curvature, helical twisting, etc.) will cause a change in the electrostatic potential of the DNA molecule and may thereby affect the search dynamics of DBPs that interact non-specifically with DNA by making their charged recognition region to penetrate into the DNA major grooves.

Protein dynamics on linear and circular DNA as a function of salt concentration

Characterizing the dynamics of the protein–DNA bound state, which is governed by non-specific electrostatic interac-

tions, requires finding a suitable salt condition at which the protein remains in the close vicinity of the DNA molecule and interacts with it. To this end, we performed coarse-grained molecular dynamics simulations of Sap-1 paired with linear B-DNA and circular DNA, separately, under a wide range of salt concentrations (0.02–0.20 M) and presented the population of the different search modes (sliding, hopping and 3D diffusion (see Materials and Methods section)) as a function of salt concentration in Figure 2A and B, respectively.

Though the relative populations of the three search modes vary between linear and circular DNA, in both cases the sliding propensity decreases and 3D diffusion increases with increasing salt concentrations. Higher salt concentrations weaken the electrostatic attractions between the DBP and DNA, allowing DBPs to dissociate from DNA more easily. The hopping mode, characterized by protein configurations that are not too close to the DNA but still bound to it (see Materials and Methods section), is most populated at moderate salt concentrations ($Cs = 0.08$ M). A suitable choice of salt condition at which Sap-1 remains associated with both linear and circular DNA is 0.02 M (3D diffusion at this concentration is only ~1%); at this concentration, the DBP performs either sliding or hopping along the DNA contour irrespective of the DNA structure.

Role of DNA curvature in DBP dynamics

Having identified the salt condition that is adequate to probe the bound state dynamics of the Sap-1-DNA complex, we then investigated the effect of DNA curvature on protein search dynamics. We asked how the variation in electrostatic potential and major groove widths (caused by the DNA curvature) between the interior and exterior of the molecule (ΔEP and ΔW, respectively) affect the search mechanism by which DPBs scan DNA. To answer this question, we performed extensive molecular dynamics simulations of the Sap-1 protein with each of the 15 circular DNA (circumference, 50–500 bp) at the 0.02 M salt condition. The position of Sap-1 with respect to the circular DNA was further characterized by determining whether the distance from the center of the recognition helix of Sap-1 to the center of the DNA circle was less than the associated DNA radius, in which case the protein was classified as lying inside the DNA circle, or greater than the DNA radius, in which case the protein was considered to lie outside the circle.

Figure 3A presents the propensities for sliding, hopping and 3D diffusion as a function of the difference between the external and internal major groove widths (ΔW), by analyzing all configurations of Sap-1 that are sampled during our simulations. We found that sliding frequency decreases while hopping propensity increases at high ΔW (which corresponds to high DNA curvature) values. This is because, as curvature increases, ΔEP increases (ΔEP $\geq 5.0 \, k_BT$ for $\Delta W \geq 1.8$ Å), which makes it more difficult for the protein to slide from the inside to the outside of the DNA circle. In this context, one should note that the suggested average free energy barrier for sliding dynamics by DBPs is only $-1.1 \pm 0.2 \, k_BT$ (18). On the other hand, inside the highly curved DNA structures, the close proximity of the negative charges on the DNA backbone promotes hopping, as can be seen

from the steep rise in hopping frequency inside the DNA at high ΔW values (Figure 3B). This result is consistent with the study of Broek *et al.*, who, using optical tweezers and a fast buffer exchange system, observed an enhanced hopping frequency for EcoRV on coiled DNA (higher curvature) compared with a linear DNA structure (79).

Efficiency of DNA search varies with DNA curvature

Furthermore, alterations in the DNA search mechanism adopted in response to changes in the curvature of DNA may also play a major role in determining the efficiency of the search, which can be defined as the number of DNA base pairs visited by sliding dynamics. In a recent theoretical study, Givaty and Levy investigated (26) the search efficiency of DBPs as a function of salt concentration and suggested that, while sliding is a prerequisite for many specific protein–DNA recognitions, this mode of transport is typically slow. Therefore, for facilitated diffusion, the hopping mode, which helps DBPs to move linearly on the DNA contour, could be beneficial. In fact, that work identified that the optimum search efficiency for a protein can be attained when sliding constitutes merely 20% of the total search. This observation was in line with the study by Berg *et al.* (6). Nevertheless, it is expected that, for different proteins, different ratios between the sliding and hopping modes should be used to achieve an optimal search. Here, we ask whether the DNA search efficiency of proteins changes with DNA curvature.

We addressed this question by estimating the number of positions probed by Sap-1 during the simulations using sliding dynamics (26). In addition, we measured D1 from the linear behavior of the mean square displacement along the DNA contour (see Materials and Methods section) of Sap-1 using only the sliding search mode or a combination of sliding and hopping. The results are presented in Figure 4 as a function of ΔW. For DNA with $0 \leq \Delta W < 1.8$ Å (corresponds to circular DNA with $100 < N_{bp} \leq 500$; i.e. for minimally curved DNA structures), the number of visited sites shows a roughly constant value of 50–70. This means that Sap-1 scanned all these DNA molecules with roughly the same efficiency. However, in highly curved DNA minicircles, where $\Delta W \geq 1.8$ Å ($N_{bp} \leq 100$), the number of probed positions decreases sharply because of a decrease in the use of sliding (Figure 3B), even though hopping-assisted diffusion (green line Figure 4B) increases along the DNA contour. Therefore, the optimal search efficiency was achieved for $\Delta W \sim 2.1$ Å (the curvature of the corresponding DNA is 0.02 per Å), where Sap-1 diffuses relatively fast (D1 = 4.43 Å^2/time step) by hopping yet scanned ~62 bp (out of 90) by sliding. When ΔW values are too small or large, which corresponds to very low or high curvatures, the result is either very fast diffusion without binding the DNA base pairs tightly (i.e. without sliding) or slow diffusion with repeated visits to the same DNA sites.

Searching circular DNA with various curvatures

To examine the mode of interaction of Sap-1 with DNA molecules of different curvatures, we monitored the Cartesian coordinates of the center of the recognition helix of
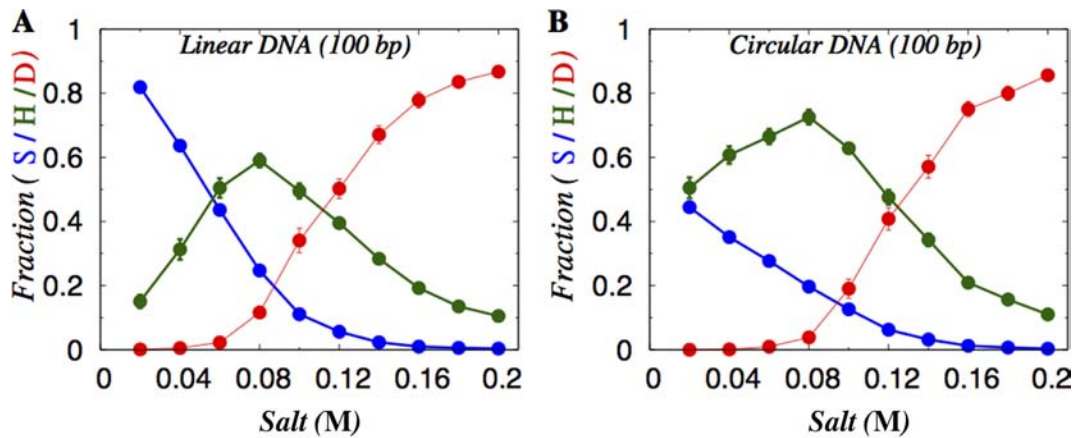
Figure 2. Effect of salt concentration on the interplay between sliding (S), hopping (H) and 3D diffusion (D) for the Sap1 protein on (**A**) linear DNA molecule of length 100 bp and (**B**) circular DNA molecule with circumference 100 bp.
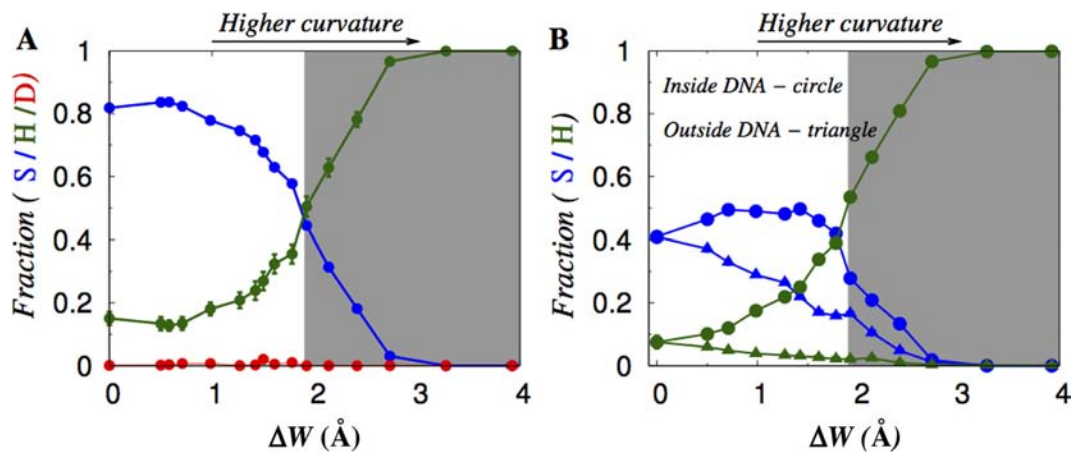

Figure 3. Effect of DNA curvature on DBP search dynamics. (**A**) Proportion of sliding (S), hopping (H) and 3D diffusion (D) dynamics adopted by the DBP as a function of the difference between the widths of exterior and interior major grooves (ΔW; caused by changes in DNA curvature) for circular DNA molecules (circumference, 50–500 bp) at 0.02 M salt concentration. (**B**) Sliding and hopping dynamics are further characterized depending on the position of Sap-1 with respect to circular DNA. Triangles and circles represent the fraction of sliding and hopping events during which the protein is located outside and inside of the circular DNA, respectively. Gray shaded region denotes DNA minicircles of circumference ≤ 100 bp (also characterized by large DNA curvatures).

Sap-1 during all 10 coarse-grained simulations. Figure 5 portrays the path for sliding dynamics (cyan) of Sap-1 on DNA with a circumference of 200, 100, 70 or 60 bp. While, on a circular DNA molecule with a circumference of 100 bp (or higher), sliding is strongly coupled with rotations around the DNA major grooves, frequent disruptions in rotation can be observed in highly curved DNA circles (N_{bp} < 70). Upon a further increase in curvature (N_{bp} = 60), sliding dynamics is completely switched off and only hopping (green dots) exists. This is also evident in the E_{DH}–R free-energy surfaces (Figure 6), where the two minima representing sliding and hopping dynamics on 100 bp circular DNA shift to a single pronounced minimum for hopping on 60 bp circular DNA. The associated drop in Debye–Hückel energy, E_{DH} reflects the strong electrostatic attractions between the positively charged recognition helix of Sap-1 and the negatively charged phosphate atoms of DNA, which effectively confines Sap-1 inside the DNA core, allowing it to perform only hopping dynamics. It should be noted, how-

ever, that such DNA minicircles (N_{bp} < 70) tend to be unstable *in vivo* and likely to form sharp kinks in order to release large strain due to high DNA curvature.

Effect of DNA helical twisting on dynamics of DBPs

The geometry of DNA conformations can be affected not only by DNA curvature but also by its degree of twisting in the DNA double helix. We note that, in a relaxed double helical B-DNA molecule, the two strands twist around the helical axis typically once every 10.4–10.5 bp of sequence. Further increase or decrease in the number of helical twists, as some enzymes can do, strains the conformation of the DNA. The strain is typically relieved by the adoption of a new shape, commonly referred to as a DNA supercoil. Here, by varying the change in linking number, Δlk, between −2 and 5, we generated eight circular DNA conformations with varying degree of helical twist. We assumed that, despite adding or subtracting moderate number of twists, our closed DNA structures could still exist in the
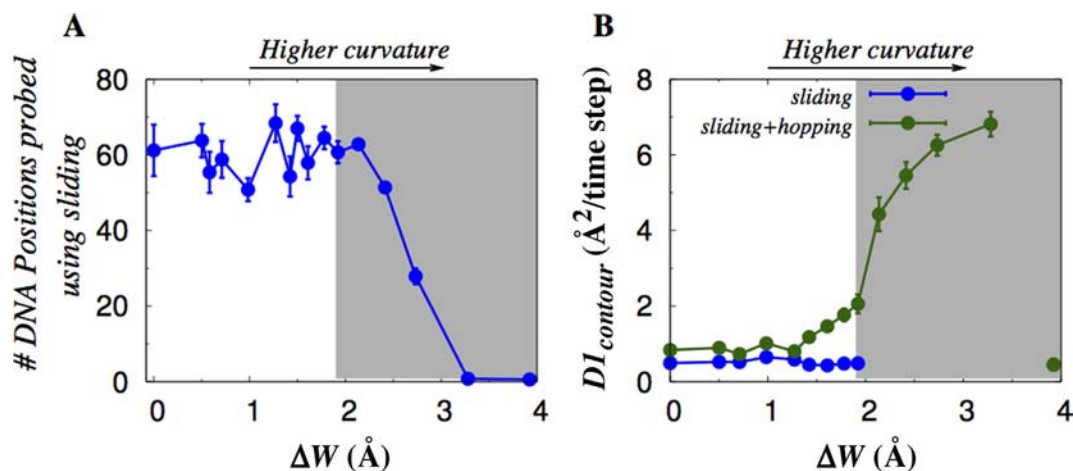
Figure 4. Role of DNA curvature in determining the efficiency of DNA search performed by Sap-1 at $Cs = 0.02$ M. (**A**) The efficiency is measured by the number of base pairs probed by Sap-1 using sliding dynamics during the simulation and presented as a function of the difference between the outer and inner major groove widths, ΔW (caused by changes in DNA curvature). (**B**) The one-dimensional diffusion coefficient D_1 calculated for the portions of the simulation during which Sap-1 scanned the DNA contour via pure sliding (blue circles) and for the portions during which Sap-1 was bound to the DNA (green circles) by either the sliding or hopping modes of dynamics. As sliding frequency decreases sharply for $\Delta W \geq 1.8$ Å, D_1 values were not calculated beyond this point. The extreme right point (close to $\Delta W = 4.0$) is an outlier, which represents the results for a circular DNA with a circumference of 50 bp. The inner core of this DNA is smaller than the size of Sap-1, which forces Sap-1 to diffuse freely and prevents sliding and hopping interactions. Gray shaded region denotes DNA minicircles of circumference ≤ 100 bp.
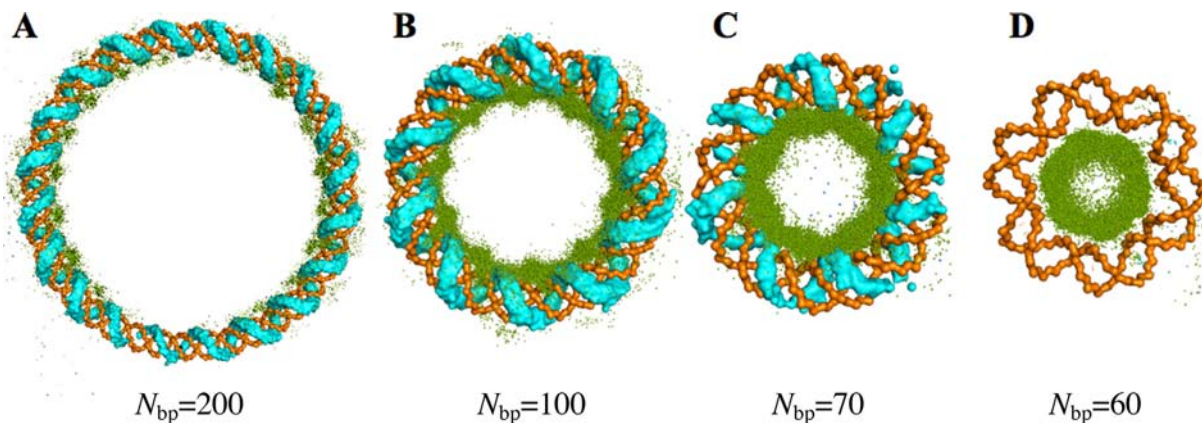

Figure 5. Trace of the search path of Sap1 around circular DNA of circumference (**A**) 200 bp, (**B**) 100 bp, (**C**) 70 bp and (**D**) 60 bp at 0.02 M salt concentration. DNA is colored orange, while cyan and green represent the sliding and hopping modes, respectively. The low salt concentration causes 3D diffusion events to occur only very rarely, which facilitates characterization of the bound protein–DNA state.

relaxed planar circular form and no writhing would take place. Such an assumption is valid only at very low salt concentration (80) limit (note that we also set a low salt condition, $Cs = 0.02$ M), although, for severely over- or under-twisted DNA structures, the strain is too large to maintain the circular form. In fact, these DNA structures are bound to adopt more compact, supercoiled conformations in order to release the strain. Nevertheless, the present assumption to represent over- and under-twisted DNA in relaxed circular form is helpful to isolate the effects of helical twisting in DNA on protein dynamics and also relevant to understand the changes in DNA conformation on a local scale, i.e. in terms of groove geometry.

Our results suggest that, as the degree of twisting in DNA double helix increases, DNA curvature increases only slightly (Supplementary Figure S3), but W_{in} decreases considerably (Figure 7A). Particularly narrow major grooves arise in order to accommodate the extra turns caused by an increase in the Δlk values. As a result, negatively charged phosphate atoms on the DNA back bone tend to cluster inside the circular DNA, giving rise to a strong electrostatic potential (EP_{in} in Figure 7B). The corresponding effects on protein search dynamics are shown in Figure 7C, which presents the sliding and hopping propensities as a function of Δlk. The result implies that sliding is most preferred in under-twisted DNA structures ($\Delta lk = -2$, see Figure 8), whose major groves are sufficiently wide to admit Sap-1. With further under-twisting ($\Delta lk = -5$), DNA unwinds considerably and both major and minor grooves become comparably wider, and thus equally compatible with sliding by Sap-1 (Figure 8). Although such a DNA conformation is compatible with sliding; the overall scanning of the DNA contour is extremely slow because of the typically slow nature of the sliding dynamics (characterized by
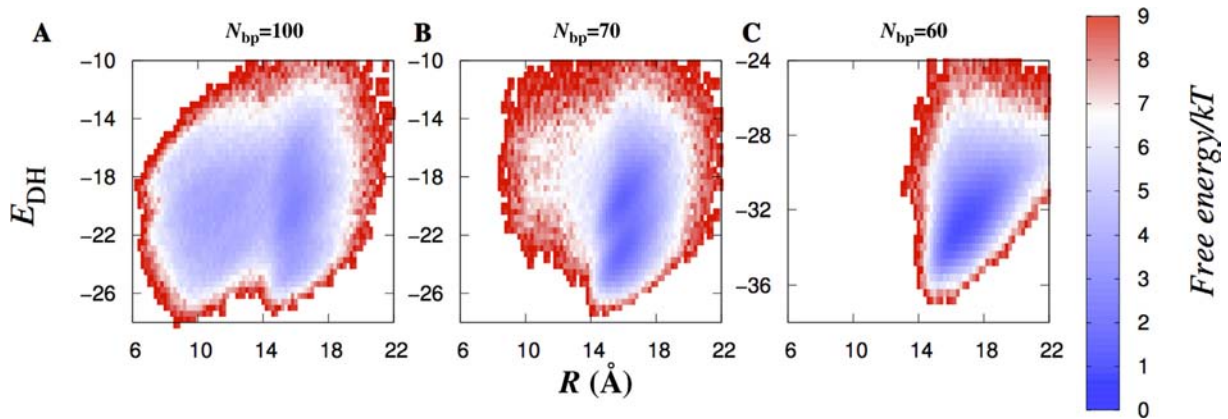
Figure 6. Free-energy surfaces $F(E_{DH}, R)$ for circular DNA structures of circumference (**A**) 100 bp, (**B**) 70 bp and (**C**) 60 bp, where E_{DH} is the electrostatic energy calculated using Debye–Hückel relations (see Materials and Methods section) at a salt concentration of 0.02 M. R represents the distance between the center of mass of the recognition helix of Sap-1 and the center of the closest base pairs in the circular DNA. Therefore, minima correspond to a small R, which denotes sliding, whereas the existence of hopping dynamics can be found at higher R. kT denotes Boltzmann constant times temperature, where the temperature is set such that Sap-1 is in a fully folded state during the simulations.
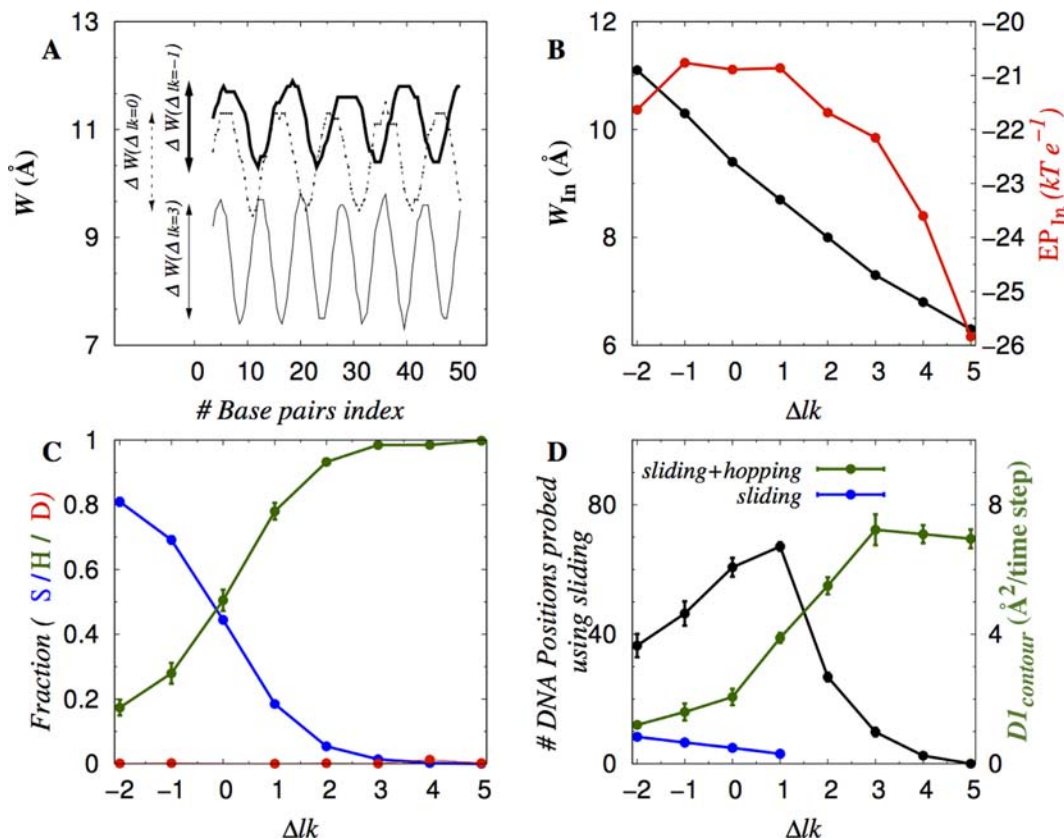

Figure 7. Role of DNA supercoiling on search dynamics of DBPs. (**A**) Variation in major groove width for minicircle DNA with linking number (Δlk) of -1, 0 and 3. (**B**) Major groove widths located inside the DNA circle (W_{in}) and the associated electrostatic potential (EP$_{in}$) are presented as a function of change in linking number (Δlk) (and, hence, as a function of W_{in}) in circular DNA at $Cs = 0.02$ M. (**C**) Number of base pairs probed by Sap-1 using sliding, hopping and 3D diffusion dynamics on 100 bp circular DNA conformations with varying numbers of helical twists (Δlk). (**D**) Diffusion coefficient (D$_1$) calculated for the portions of the simulation during which Sap-1 scanned the DNA contour via pure sliding (blue circles) and for the portions during which Sap-1 was bound to the DNA (green circles) by either the sliding or hopping mode of dynamics. As sliding frequency decreases sharply for $\Delta lk \geq 1$, D1 values were not calculated beyond this point.
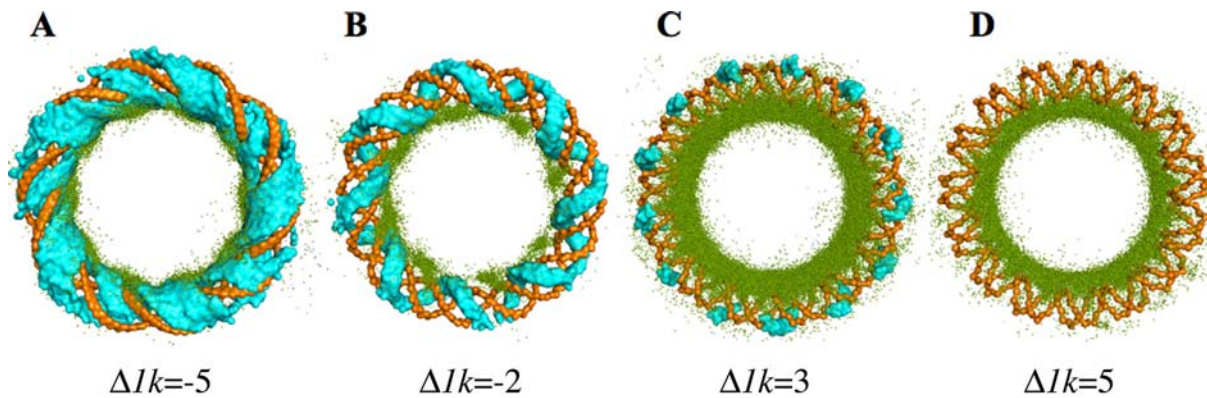
Figure 8. Traces of the search path of Sap-1 on 100 bp circular DNA twisted to various extents around the double helix. A DNA conformation with $\Delta lk < 0$ denotes an under-twisted DNA structure having wider internal groove widths into which DBPs fit easily to perform smooth sliding. A DNA conformation with $\Delta lk > 0$ represents an over-twisted structure. With increasing DNA twisting, groove widths become narrower and therefore prevent sliding dynamics by not allowing DBPs to fit well inside the major groove.

low D1 values, blue line in Figure 7D). The hopping mode of dynamics, however, increases (Figure 7C) with increased helical twisting, Δlk (also see $\Delta lk = 3$ and $\Delta lk = 5$ in Figure 8). This is because of the highly negative electrostatic potential inside the major groove of the over-twisted DNA. Up to a certain point (beyond which the DBP cannot enter the DNA major groove) the highly negative interior electrostatic potential acts as a promoter of hopping events as it is strong enough to enable mild attraction between DBP and DNA, but not so strong as to prevent dissociation of the DBP from the DNA surface. Hopping dynamics might be useful (green line in Figure 7D) to accelerate the diffusion of Sap-1 along the DNA contour, however, an optimal search efficiency can only be attained while both sliding and hopping operate synergistically such that the protein can diffuse rapidly along the DNA contour yet scan many DNA base pairs through sliding. Here, we found (in Figure 7D) that Sap-1 can scan a maximum number of base pairs (~ 67 bp out of 100) in circular DNA when the DNA is slightly over-twisted ($\Delta lk = 1$). Optimal efficiency is achieved through 78% hopping (fast diffusion, D1 ~ 3.88 Å^2/time step) and only 18% sliding dynamics (Figure 7C; the values corresponding to $\Delta lk = 1$).

CONCLUSIONS

In this study, we demonstrated that the strength and nature of the non-specific electrostatic interactions that govern the search dynamics of DBPs are strongly correlated with the conformation of the DNA. To achieve this, we tuned two structural parameters, namely curvature and the extent of helical twisting in circular DNA. These two factors are mutually independent of each other and so are their effects in shaping the major groove widths and the electrostatic potential around the DNA molecules. Increasing the curvature enhances the differences in major groove widths (ΔW) and electrostatic potential (ΔEP) between the exterior and interior of the circular DNA. An increase in DNA helical twisting, obtained by adding additional helical twists to a fixed DNA circumference, however, leads to a decrease in the interior major groove widths (W_{in}). As a result, the strength of the electrostatic potential increases such that ΔEP remains

roughly constant. Such modulation in electrostatic potential through changing the geometry of the circular DNA conformation results in markedly different search dynamics for DBPs on circular compared with linear B-DNA.

Of course, the relative weights of the various search mechanisms are also dependent on the sequence composition and structural features of DBPs (28,32,81). Our results suggest that, for a given DBP, the rotation-coupled sliding dynamics is precluded in highly curved DNA because of the large electrostatic energy barrier between the inside and outside of the DNA molecule. Under such circumstances, proteins prefer to hop in order to explore interior DNA sites. This result is consistent with the experimental observation of Broek *et al.* (82), who has observed almost twice the number of hopping events compared with sliding on a coiled DNA conformation under suitable salt conditions. A similar drop in sliding propensity is also found if the number of helical twists in the DNA structure increases. Additional turns in the DNA molecules are accommodated at the cost of narrowing the major groove widths to such an extent that they can no longer accommodate the recognition surface of DBPs during sliding dynamics. As an alternative search mode, the increased electrostatic potential inside the curved DNA surface promotes hopping events.

The change in the DNA search mechanism adopted by DBPs as a result of changes in the geometry of DNA conformations also has far reaching implications for determining the efficiency of the search process, which is defined by the number of new DNA base pair sites visited. Based on our coarse-grained molecular dynamics simulations, we found that the search process is not just naive 1D sliding, but rather a delicately weighted mixture of sliding and hopping (and other modes of dynamics). While sliding promotes scanning of the DNA sites by allowing proteins to bind tightly with DNA, hopping accelerates the linear diffusion of the protein (corresponding to high D1 values) along the DNA contour. Since both transport modes are strongly connected with DNA geometry, the optimal search efficiency is also largely dependent on the conformational features of DNA molecules. An aspect that remained to be addressed in the future deals with the interplay between the

internal flexibility of the DNA and the populations of the search modes.

SUPPLEMENTARY DATA

Supplementary Data are available at NAR Online.

REFERENCES

1. Lavery,R. and Zakrzewska,K. (2012) Towards a molecular view of transcriptional control. *Curr. Opin. Struct. Biol.*, **22**, 160–167.
2. Garvie,C.W. and Wolberger,C. (2001) Recognition of specific DNA sequences. *Mol. Cell*, **8**, 937–946.
3. von Hippel,P.H. (2007) From 'simple' DNA–protein interactions to the macromolecular machines of gene expression. *Annu. Rev. Biophys. Biomol. Struct.*, **36**, 79–105.
4. Riggs,A., Bourgeous,S. and Cohn,M. (1970) The lac represser–operator interaction *1, *2III. Kinetic studies. *J. Mol. Biol.*, **53**, 401–417.
5. Halford,S.E. (2009) An end to 40 years of mistakes in DNA–protein association kinetics? *Biochem. Soc. Trans.*, **37**, 343–348.
6. Berg,O.G., Winter,R.B. and von Hippel,P.H. (1981) Diffusion-driven mechanisms of protein translocation on nucleic acids. 1. Models and theory. *Biochemistry*, **20**, 6929–6948.
7. von Hippel,P.H. and Berg,O.G. (1989) Facilitated target location in biological systems. *J. Biol. Chem.*, **264**, 675–678.
8. Gowers,D.M. and Halford,S.E. (2003) Protein motion from non-specific to specific DNA by three-dimensional routes aided by supercoiling. *EMBO J.*, **22**, 1410–1418.
9. Gowers,D.M., Wilson,G.G. and Halford,S.E. (2005) Measurement of the contributions of 1D and 3D pathways to the translocation of a protein along DNA. *Proc. Natl. Acad. Sci. U.S.A.*, **102**, 15883–15888.
10. Wang,J., Lu,Q. and Lu,H.P. (2006) Single-molecule dynamics reveals cooperative binding–folding in protein recognition. *PLoS Comput. Biol.*, **2**, e78.
11. Jeltsch,A. and Pingoud,A. (1998) Kinetic characterization of linear diffusion of the restriction endonuclease EcoRV on DNA. *Biochemistry*, **37**, 2160–2169.
12. Jeltsch,A., Wenz,C., Stahl,F. and Pingoud,A. (1996) Linear diffusion of the restriction endonuclease EcoRV on DNA is essential for the in vivo function of the enzyme. *EMBO J.*, **15**, 5104–5111.
13. Stanford,N.P., Szczelkun,M.D., Marko,J.F. and Halford,S.E. (2000) One- and three-dimensional pathways for proteins to reach specific DNA sites. *EMBO J.*, **19**, 6546–6557.
14. Stivers,J.T. and Schonhoft,J.D. (2012) Timing facilitated site transfer of an enzyme on DNA. *Nat. Chem. Biol.*, **8**, 205–210.
15. Porecha,R.H. and Stivers,J.T. (2008) Uracil DNA glycosylase uses DNA hopping and short-range sliding to trap extrahelical uracils. *Proc. Natl. Acad. Sci. U.S.A.*, **105**, 10791–10796.
16. Rowland,M.M., Schonhoft,J.D., McKibbin,P.L., David,S.S. and Stivers,J. (2014) Microscopic mechanism of DNA damage searching by hOGG1. *Nucleic Acids Res.*, **45**, 9295–9303.
17. Gorman,J., Plys,A.J., Visnapuu,M.-L., Alani,E. and Greene,E.C. (2010) Visualizing one-dimensional diffusion of eukaryotic DNA repair factors along a chromatin lattice. *Nat. Struct. Mol. Biol.*, **17**, 932–938.
18. Blainey,P.C., Luo,G., Kou,S.C., Mangel,W.F., Verdine,G.L., Bagchi,B. and Xie,X.S. (2009) Nonspecifically bound proteins spin while diffusing along DNA. *Nat. Struct. Mol. Biol.*, **16**, 1224–1229.
19. Bustamante,C. (1999) Facilitated target location on DNA by individual *Escherichia coli* RNA polymerase molecules observed with the scanning force microscope operating in liquid. *J. Biol. Chem.*, **274**, 16665–16668.
20. Elf,J., Li,G.-W. and Xie,X.S. (2007) Probing transcription factor dynamics at the single-molecule level in a living cell. *Science*, **316**, 1191–1194.
21. Graneli,A., Yeykal,C.C., Robertson,R.B. and Greene,E.C. (2006) Long-distance lateral diffusion of human Rad51 on double-stranded DNA. *Proc. Natl. Acad. Sci. U.S.A.*, **103**, 1221–1226.
22. Iwahara,J. and Clore,G.M. (2006) Detecting transient intermediates in macromolecular binding by paramagnetic NMR. *Nature*, **440**, 1227–1230.
23. Iwahara,J. and Clore,G.M. (2006) Direct observation of enhanced translocation of a homeodomain between DNA cognate sites by NMR exchange spectroscopy. *J. Am. Chem. Soc.*, **128**, 404–405.
24. Iwahara,J., Zweckstetter,M. and Clore,G.M. (2006) NMR structural and kinetic characterization of a homeodomain diffusing and hopping on nonspecific DNA. *Proc. Natl. Acad. Sci. U.S.A.*, **103**, 15062–15067.
25. Marcovitz,A. and Levy,Y. (2011) Frustration in protein–DNA binding influences conformational switching and target search kinetics. *Proc. Natl. Acad. Sci. U.S.A.*, **108**, 17957–17962.
26. Givaty,O. and Levy,Y. (2009) Protein sliding along DNA: dynamics and structural characterization. *J. Mol. Biol.*, **385**, 1087–1097.
27. Chen,C. and Pettitt,B.M. (2011) The binding process of a nonspecific enzyme with DNA. *Biophys. J.*, **101**, 1139–1147.
28. Vuzman,D. and Levy,Y. (2010) DNA search efficiency is modulated by charge composition and distribution in the intrinsically disordered tail. *Proc. Natl. Acad. Sci. U.S.A.*, **107**, 21004–21009.
29. Vuzman,D. and Levy,Y. (2012) Intrinsically disordered regions as affinity tuners in protein–DNA interactions. *Mol. Biosyst.*, **8**, 47–57.
30. Khazanov,N. and Levy,Y. (2011) Sliding of p53 along DNA can be modulated by its oligomeric state and by cross-talks between its constituent domains. *J. Mol. Biol.*, **408**, 335–355.
31. Vuzman,D., Polonsky,M. and Levy,Y. (2010) Facilitated DNA search by multidomain transcription factors: cross talk via a flexible linker. *Biophys. J.*, **99**, 1202–1211.
32. Khazanov,N., Marcovitz,A. and Levy,Y. (2013) Asymmetric DNA-search dynamics by symmetric dimeric proteins. *Biochemistry*, **52**, 5335–5344.
33. Guardiani,C., Cencini,M. and Cecconi,F. (2014) Coarse-grained modeling of protein unspecifically bound to DNA. *Phys. Biol.*, **11**, 026003–026014.
34. Brackley,C., Cates,M. and Marenduzzo,D. (2013) Intracellular facilitated diffusion: searchers, crowders, and blockers. *Phys. Rev. Lett.*, **111**, 108101–108105.
35. Marklund,E.G., Mahmutovic,A., Berg,O.G., Hammar,P., van der Spoel,D., Fange,D. and Elf,J. (2013) Transcription-factor binding and sliding on DNA studied using micro- and macroscopic models. *Proc. Natl. Acad. Sci. U.S.A.*, **110**, 19796–19801.
36. Zabet,N.R. and Adryan,B. (2012) Computational models for large-scale simulations of facilitated diffusion. *Mol. Biosyst.*, **8**, 2815–2827.
37. Chu,X., Liu,F., Maxwell,B.A., Wang,Y., Suo,Z., Wang,H., Han,W. and Wang,J. (2014) Dynamic conformational change regulates the protein–DNA recognition: An investigation on binding of a Y-family polymerase to its target DNA. *PLoS Comput. Biol.*, **10**, e1003804.
38. Slutsky,M. and Mirny,L.A. (2004) Kinetics of protein–DNA interaction: facilitated target location in sequence-dependent potential. *Biophys. J.*, **87**, 4021–4035.
39. Kolomeisky,A.B. (2011) Physics of protein–DNA interactions: mechanisms of facilitated target search. *Phys. Chem. Chem. Phys.*, **13**, 2088–2095.
40. Dahirel,V., Paillusson,F., Jardat,M., Barbi,M. and Victor,J.-M. (2009) Nonspecific DNA–protein interaction: why proteins can diffuse along DNA. *Phys. Rev. Lett.*, **102**, 228101–228101.
41. Bénichou,O., Kafri,Y., Sheinman,M. and Voituriez,R. (2009) Searching fast for a target on DNA without falling to traps. *Phys. Rev. Lett.*, **103**, 138102.

42. Klenin,K.V., Merlitz,H., Langowski,J. and Wu,C.X. (2006) Facilitated diffusion of DNA-binding proteins. *Phys. Rev. Lett.*, **96**, 018101–018104.

43. Veksler,A. and Kolomeisky,A.B. (2013) Speed-selectivity paradox in the protein search for targets on DNA: is it real or not? *J. Phys. Chem. B*, **117**, 12695–12701.

44. Hu,T., Grosberg,A.Y. and Shklovskii,B.I. (2006) How proteins search for their specific sites on DNA: the role of DNA conformation. *Biophys. J.*, **90**, 2731–2744.

45. Brackley,C.a., Cates,M.E. and Marenduzzo,D. (2013) Effect of DNA conformation on facilitated diffusion. *Biochem. Soc. Trans.*, **41**, 582–588.

46. Prevost,C., Takahashi,M. and Lavery,R. (2009) Deforming DNA: from physics to biology. *Chemphyschem*, **10**, 1399–1404.

47. Fogg,J.M., Randall,G.L., Pettitt,B.M., Sumners de,W.L., Harris,S.A. and Zechiedrich,L. (2012) Bullied no more: when and how DNA shoves proteins around. *Q. Rev. Biophys.*, **45**, 257–299.

48. Bouvier,B., Zakrzewska,K. and Lavery,R. (2011) Protein–DNA recognition triggered by a DNA conformational switch. *Angew. Chem. Int. Ed.*, **50**, 6516–6518.

49. Bouvier,B. and Lavery,R. (2009) A free energy pathway for the interaction of the SRY protein with its binding site on DNA from atomistic simulations. *J. Am. Chem. Soc.*, **131**, 9864–9865.

50. Chen,Z., Yang,H. and Pavletich,N.P. (2008) Mechanism of homologous recombination from the RecA-ssDNA/dsDNA structures. *Nature*, **453**, 489–484.

51. Luger,K., Mäder,A.W., Richmond,R.K., Sargent,D.F. and Richmond,T.J. (1997) Crystal structure of the nucleosome core particle at 2.8 A resolution. *Nature*, **389**, 251–260.

52. Halford,S.E. and Marko,J.F. (2004) How do site specific DNA binding proteins find their targets? *Nucleic Acids Res.*, **32**, 3040–3052.

53. Rohs,R., West,S.M., Liu,P. and Honig,B. (2009) Nuance in the double-helix and its role in protein–DNA recognition. *Curr. Opin. Struct. Biol.*, **19**, 171–177.

54. Barozzi,I., Simonatto,M., Bonifacio,S., Yang,L., Rohs,R., Ghisletti,S. and Natoli,G. (2014) Coregulation of transcription factor binding and nucleosome occupancy through DNA features of mammalian enhancers. *Mol. Cell*, **54**, 844–857.

55. Zhou,T., Yang,L., Lu,Y., Dror,I., Dantas Machado,A.C., Ghane,T., Di Felice,R. and Rohs,R. (2013) DNAshape: a method for the high-throughput prediction of DNA structural features on a genomic scale. *Nucleic Acids Res.*, **41**, W56–W62.

56. Alsallaq,R. and Zhou,H.-X. (2008) Protein association with circular DNA: rate enhancement by nonspecific binding. *J. Chem. Phys.*, **128**, 115108.

57. Rohs,R., West,S.M., Sosinsky,A., Liu,P., Mann,R.S. and Honig,B. (2009) The role of DNA shape in protein–DNA recognition. *Nature*, **461**, 1248–1253.

58. Rohs,R., Jin,X., West,S.M., Joshi,R., Honig,B. and Mann,R.S. (2010) Origins of specificity in protein–DNA recognition. *Annu. Rev. Biochem.*, **79**, 233–269.

59. Mor,A., Ziv,G. and Levy,Y. (2008) Simulations of proteins with inhomogeneous degrees of freedom: the effect of thermostats. *J. Comput. Chem.*, **29**, 1992–1998.

60. Terakawa,T., Kenzaki,H. and Takada,S. (2012) p53 searches on DNA by rotation-uncoupled sliding at C-terminal tails and restricted hopping of core domains. *J. Am. Chem. Soc.*, **134**, 14555–14562.

61. Clementi,C., Nymeyer,H. and Onuchic,J.N. (2000) Topological and energetic factors: what determines the structural details of the transition state ensemble and 'en-route' intermediates for protein folding? An investigation for small globular proteins. *J. Mol. Biol.*, **298**, 937–953.

62. Onuchic,J.N. and Wolynes,P.G. (2004) Theory of protein folding. *Curr. Opin. Struct. Biol.*, **14**, 70–75.

63. Azia,A. and Levy,Y. (2009) Nonnative electrostatic interactions can modulate protein folding: molecular dynamics with a grain of salt. *J. Mol. Biol.*, **393**, 527–542.

64. Schlick,T. (2000) Molecular Modeling and Simulation: An Interdisciplinary Guide. 2nd edn. Springer, NY.

65. Marcovitz,A. and Levy,Y. (2012) Sliding Dynamics along DNA: A Molecular Perspective. RSC, Cambridge, **10**, pp. 236–262.

66. Marcovitz,A. and Levy,Y. (2013) Obstacles may facilitate and direct DNA search by proteins. *Biophys. J.*, **104**, 2042–2050.

67. Hyeon,C. and Thirumalai,D. (2005) Mechanical unfolding of RNA hairpins. *Proc. Natl. Acad. Sci. U.S.A.*, **102**, 6789–6794.

68. Biyun,S., Cho,S.S. and Thirumalai,D. (2011) Folding of human telomerase RNA pseudoknot using ion-jump and temperature-quench simulations. *J. Am. Chem. Soc.*, **133**, 20634–20643.

69. Pincus,D.L., Cho,S.S., Hyeon,C. and Thirumalai,D. (2008) Minimal models for proteins and RNA from folding to function. *Prog. Mol. Biol. Transl. Sci.*, **84**, 203–250.

70. Schlick,T. and Perisic,O. (2009) Mesoscale simulations of two nucleosome-repeat length oligonucleosomes. *Phys. Chem. Chem. Phys.*, **11**, 10729–10737.

71. Levy,Y., Onuchic,J.N. and Wolynes,P.G. (2007) Fly-casting in protein–DNA binding: frustration between protein folding and electrostatics facilitates target recognition. *J. Am. Chem. Soc.*, **129**, 738–739.

72. Marcovitz,A. and Levy,Y. (2009) Arc-repressor dimerization on DNA: folding rate enhancement by colocalization. *Biophys. J.*, **96**, 4212–4220.

73. Li,R.Z., Ge,H.M.W. and Cho,S.S. (2013) Sequence-dependent base-stacking stabilities guide tRNA folding energy landscapes. *J. Phys. Chem. B*, **117**, 12943–12952.

74. Zheng,G., Lu,X.-J. and Olson,W.K. (2009) Web 3DNA—a web server for the analysis, reconstruction, and visualization of three-dimensional nucleic-acid structures. *Nucleic Acids Res.*, **37**, W240–W246.

75. Case,T.M.a.D.A. (1998) Modeling unusual nucleic acid structures In: Leontis,NB and SantaLucia,J, (eds). Molecular Modeling of Nucleic Acids. American Chemical Society, Washington, DC, **24**, pp. 379–393.

76. Lavery,R., Moakher,M., Maddocks,J.H., Petkeviciute,D. and Zakrzewska,K. (2009) Conformational analysis of nucleic acids revisited: curves+. *Nucleic Acids Res.*, **37**, 5917–5929.

77. Li,L., Li,C., Sarkar,S., Zhang,J., Witham,S., Zhang,Z., Wang,L., Smith,N., Petukh,M. and Alexov,E. (2012) DelPhi: a comprehensive suite for DelPhi software and associated resources. *BMC Biophys.*, **5**, 9.

78. Lindorff-Larsen,K., Piana,S., Palmo,K., Maragakis,P., Klepeis,J.L., Dror,R.O. and Shaw,D.E. (2010) Improved side-chain torsion potentials for the Amber ff99SB protein force field. *Proteins*, **78**, 1950–1958.

79. Van Den Broek,B., Lomholt,M.A., Kalisch,S.M.J., Metzler,R. and Wuite,G.J.L. (2008) How DNA coiling enhances target localization by proteins. *Proc. Natl. Acad. Sci. U.S.A.*, **105**, 15738–15742.

80. Schlick,T., Li,B. and Olson,W.K. (1994) The influence of salt on the structure and energetics of supercoiled DNA. *Biophys. J.*, **67**, 2146–2166.

81. Vuzman,D., Azia,A. and Levy,Y. (2010) Searching DNA via a 'Monkey Bar' mechanism: the significance of disordered tails. *J. Mol. Biol.*, **396**, 674–684.

82. van den Broek,B., Lomholt,M.A., Kalisch,S.-M.J., Metzler,R. and Wuite,G.J.L. (2008) How DNA coiling enhances target localization by proteins. *Proc. Natl. Acad. Sci. U.S.A.*, **105**, 15738–15742.